Azimuthal Variation of the Emissivity of Foam From C and X Band Polarimetric Measurements

L. A. Rose, J. P. Bobak, and P. W. Gaiser
Naval Research Laboratory, Washington, DC
M. D. Anguelova
NRC Research Associate
D. J. Dowgiallo
Interferometrics, Inc.
W. E. Asher
Applied Physics Laboratory, University of Washington, Seattle
S. C. Reising and S. Padmanabhan
Colorado State University

***Abstract*-Sea foam increases surface emission and brightness temperature at microwave frequencies. Together with the surface roughness, it is a key component of the signal used to obtain surface wind vector with satellite-borne radiometric and polarimetric instruments. Current knowledge of foam emissivity, however, is incomplete, particularly in regard to azimuthal effects.**

Since breaking waves on the open ocean are intermittent and highly variable, radiometric measurements of reproducible breaking waves were performed in an outdoor salt water wave tank in 2002 and 2004. The wave tank was configured to create foam-producing breaking waves using an underwater shoaling beach. Four radiometers, operating at frequencies of 6.8, 10.8, 18.7, and 37 GHz, were positioned at several incidence angles and azimuth look angles to record microwave emission from the breaking waves. A bore-sighted video camera recorded images of foam fraction within radiometers footprints. Auxiliary information on the wave field and breaking events (such as void fraction, bubble size spectrum, foam layer thickness, wave height, and subsurface turbulent dissipation) was provided by a suite of additional instruments.

The results of wave tank measurements of the azimuthal dependence of foam emissivity at 6.8 and 10.8 GHz are presented, and possible contributors to the observed azimuthal changes of foam emissivity are discussed.

Sponsored by the NPOESS Integrated Program Office

INTRODUCTION

Successful naval operations require excellent knowledge of the ocean wind speed and direction. In addition, the global ocean wind vector is a key element for weather forecasting and for climate and oceanography studies. WindSat, a satellite-borne multi-frequency polarimetric microwave radiometer developed by the Naval Research Laboratory, has demonstrated the ability to remotely sense the global ocean wind vector from space [1]. The wind direction signal measured by WindSat is about two orders of magnitude smaller than the background scene, and only a little larger than the radiometer noise floor. Therefore, any small uncertainties in the geophysical model used to retrieve the wind direction will introduce errors in the retrieved wind vector. One such uncertainty is the contribution of sea foam to the wind direction signal.

Down-looking radiometers, such as WindSat, receive energy emitted from both the ocean surface and the atmosphere. The energy from the ocean surface, quantified as the brightness temperature, is related to surface physical temperature by

$$T_B = e_S \cdot T_w$$

where T_B is the brightness temperature, T_w is the physical temperature of ocean water surface,

and e_S is surface emissivity, which depends on the measurement frequency, polarization, incidence angle, and the azimuth angle between wind direction and the direction from which observations are made. The emissivity of the sea surface also depends on physical properties of the water surface such as temperature, salinity, and surface roughness, the latter being primarily wind driven.

The presence of foam and roughness created by wind and breaking waves greatly increases the surface emission at microwave frequencies; the surface emissivity is sometimes written as

$$e_S = f \cdot e_f + (1 - f) \cdot e_r$$

where f is the fraction of the surface covered with foam, e_f is the emissivity of foam, and e_r is the emissivity of the foam-free, rough water surface. The relation of foam fraction to ocean surface wind speed has been studied by Asher et al. [2] and continues to be a topic of research interest.

Past studies of e_f, using a large area foam generator floating just beneath a calm water surface, focused on incidence angle, frequency and polarization dependencies [3], while open ocean measurements conducted from the U.S. Navy's floating instrument platform (FLIP) showed the possibility that emission due to foam depended on both incidence and azimuth angles [4]. To better understand the azimuthal dependence of e_f, the Polarimetric Observations of the Emissivity of Whitecaps EXperiment (POEWEX) was conducted in 2002 and 2004. POEWEX involved simultaneous radiometric and video measurements of breaking waves at microwave frequencies of 6.8, 10.8, 18.7, and 36.5 GHz, which match those used by WindSat and the upcoming Conical Scanning Microwave Imager/Sounder (CMIS) on the National Polar-orbiting Operational Environmental Satellite System (NPOESS).

OUTDOOR WAVETANK EXPERIMENT

Since breaking waves and foam on the open ocean are intermittent and highly variable, POEWEX was conducted under controlled conditions at the Oil and Hazardous Materials Simulated Environmental Test Tank (OHMSETT) in Leonardo, New Jersey. The outdoor saltwater wave tank, in which the salinity was controlled to 35 ppt, is 203 m long, 20 m wide, and 3.4 m deep, giving it a capacity of 3.6 million gallons. A mechanical wave generator produced waves with a period that was adjusted to be approximately 2 seconds; an artificial shoal placed in the center of the tank caused reproducible breaking waves to occur at the same location on the shoal. In situ physical measurements were performed with an underwater video camera, capacitance void fraction probes, an acoustic velocimeter, and pressure transducers. Bubble size spectra and foam thickness were characterized using the underwater camera, the void fraction probes measured the air-to-water volume ratio of the foam due to breaking waves, and wave height was inferred using the pressure transducers. These measurements provided evidence that the physical properties of the breaking waves in the tank were similar to those of breaking waves on the ocean surface. Therefore, the radiometric emission observed in the wave tank is thought to be representative of that from breaking waves in the open ocean [5].

Fig. 1 shows the experimental setup, with the radiometers suspended beneath the cradle of a boom-lift crane observing a breaking wave. The drawing shows the five azimuth angles from which observations were made at an incidence angle of 53 degrees. At incidence angles of 45 and 65 degrees, measurements were made at azimuth angles of 0, 90 and 180 degrees. A video camera bore-sighted with the radiometers provided video images from which the fractional coverage of foam in the radiometer field of view (FOV) was determined using a grayscale analysis procedure described in [6].

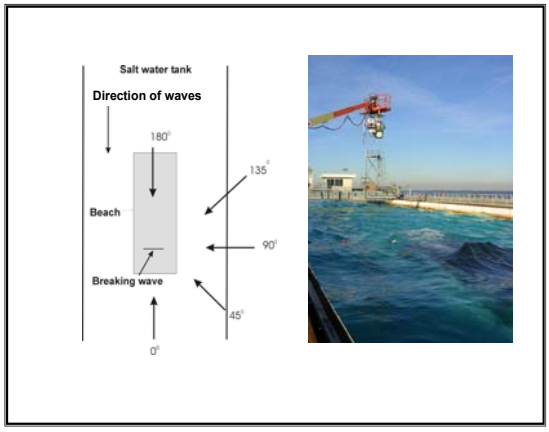

Figure 1. (left) Drawing showing azimuth angles from which observations were made and (bottom) radiometers observing waves at OHMSETT.

RADIOMETRIC MEASUREMENTS

The 6.8 GHz radiometer was operated in a total power mode while the 10.8 GHz radiometer was Dicke-switched. Radiometer specifications are given in Table 1. Calibrations were performed using external loads at ambient and liquid nitrogen temperatures; tip curves of the sky permitted the use of the 2.7 K cosmic background radiation as a second cold calibration target

The slant range distance from the radiometers to the place on the shoal where breaking waves occurred was kept at a constant value of 14 m so that changes in solid angle subtended by the area of breaking waves on the shoal was minimized when the azimuth angle or incidence angle was changed. Also, the relatively close distance of the radiometers to the target meant that the atmospheric effects of attenuation and emission of radiation could be neglected.

Measurements were made of (1) the area on the shoal where breaking waves occurred, (2) rough water away from the shoal that had no foam in the radiometer FOV, and (3) calm water when the wave generator was turned off. The calm water measurements provided a secondary calibration check on the radiometry by enabling comparison to model values of emissivity.

When the radiometers are observing the water surface in the wave tank, the measured antenna temperature is the sum of surface emission and reflected down-welling atmospheric radiation. For the two cases when antenna temperatures and foam fraction are maximum and minimum, respectively, the following two equations can be written:

TABLE 1
C AND X BAND RADIOMETER PARAMETERS

Parameter	C-band	X-band
Operation Mode	Total power	Dicke switched
Center frequency	6.8 GHz	10.8 GHz
3 dB beamwidth	9.5 degrees	7 degrees
Bandwidth	125 MHz	500 MHz
Radiometric Sensitivity (1 sec. integration time)	0.16 K	0.16 K
Absolute accuracy	1 K	2 K
Antenna side lobe level	- 23 dB	- 25 dB
Antenna main beam efficiency	95 %	95 %
Polarizations	H, V	H, V, +45, -45, left circular (L), right circular (R)

$$Ta_1 = \eta\{(f_1)[(e_f)(T_w) + (1-e_f)(T_{sky})] + (1-f_1)[(e_r)(T_W) + (1-e_r)(T_{sky})]\} + (1-\eta)T_{BACK} \quad (1)$$

and

$$Ta_2 = \eta\{(f_2)[(e_f)(T_w) + (1-e_f)(T_{sky})] + (1-f_2)[(e_r)(T_W) + (1-e_r)(T_{sky})]\} + (1-\eta)T_{BACK} \quad (2)$$

where

Ta_1 maximum value of antenna temperature when the breaking wave is in the FOV on the shoal;

f_1 maximum foam fraction when antenna temperature is a maximum value;

e_f emissivity of foam on the shoal;

Ta_2 minimum value of antenna temperature when the surface in the FOV on the shoal is mostly rough water;

f_2 minimum foam fraction when antenna temperature is a minimum value;

e_r emissivity of rough water on the shoal;

η fraction of contribution to Ta from main beam of antenna;

$(1-\eta)T_{BACK}$ contribution to Ta from outside main beam of antenna;

T_w physical temperature of the water;

T_{sky} brightness temperature of downwelling sky radiation.

Solving (1) and (2) for e_f yields:

$$e_f =$$

$$\frac{(1-f_2)(Ta_1-\eta T_{sky})-(1-f_1)(Ta_2-\eta T_{sky})}{(\eta)(f_1-f_2)(T_w-T_{sky})}$$

$$-\frac{(1-\eta)}{\eta}\frac{T_{BACK}}{T_w-T_{sky}}. \qquad (3)$$

When computing the foam emissivity using (3), measurements of the antenna temperature of rough water away from the shoal were used as an approximate value of T_{BACK}. (Note: The emissivity values shown in the plots in the following section are averages using from 50 to 180 sets of $\{Ta_1, Ta_2, f_1, f_2\}$, and the error bars are standard deviations of the average values.)

RESULTS AND DISCUSSION

Fig. 2 presents results at 53 degrees incidence angle and 90 degrees azimuth. The upper part of the figure shows video images of the breaking waves. The artificial shoal creating the breaking point is seen as a black rectangle and overlaid circles define the radiometer FOVs. The lower part of Fig. 2 plots time series of the antenna temperatures at 10.8, 18.7, and 36.5 GHz for the vertical (red) and horizontal (blue) polarizations and for the foam fraction (yellow). Maximum and minimum values of antenna temperature and foam fraction can be seen at approximately 2.5 and 4 seconds, respectively.

Figures 3 and 4 show the emissivity of foam at an incidence angle of 53 degrees as a function of azimuth angle at 6.8 and 10.8 GHz for the horizontal and vertical polarizations, respectively. At both frequencies, the plots show variation of emissivity with azimuth angle, but the variation is more pronounced for the horizontal polarization. This is the first experimental evidence of an azimuthal variation in foam emissivity.

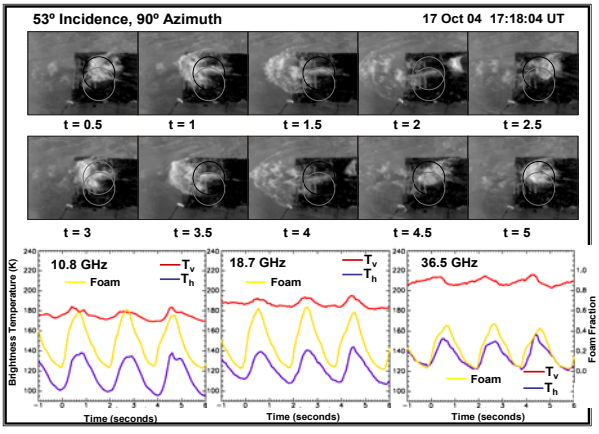

Figure 2. (top) Video images of breaking waves on the shoal in the outdoor test tank (OHMSETT) and (bottom) time series plots of antenna temperatures and foam fraction.

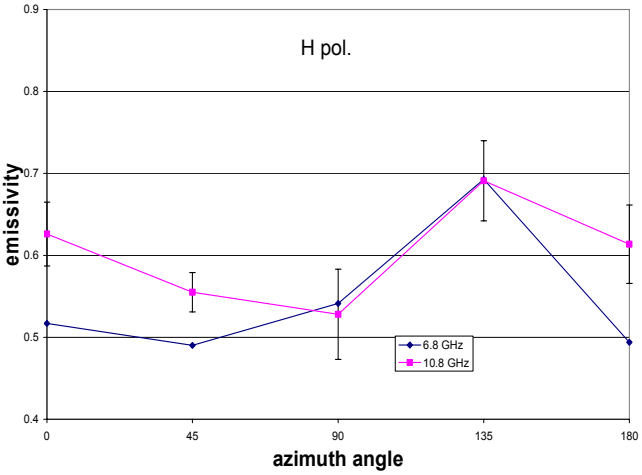

Figure 3. Foam emissivity at 6.8 and 10.8 GHz versus azimuth angle, for horizontal polarization.

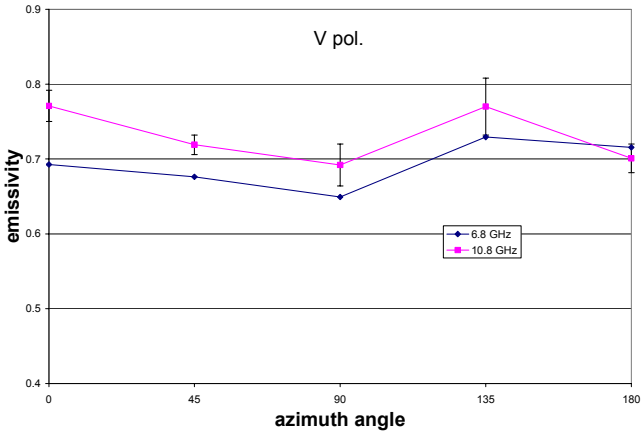

Figure 4. Emissivity of foam at 6.8 and 10.8 GHz versus azimuth angle, for vertical polarization.

Fig. 5 shows plots of emissivity versus azimuth angle for vertical, right circular (R), and horizontal polarizations, showing that the R polarization is intermediate between vertical and horizontal in displaying a variation with azimuth angle. Here the horizontal and vertical polarization data are taken from Figures 3 and 4 respectively

Azimuthal variations in foam emissivity are most probably explained by the asymmetric distribution of foam on the wave slopes. Newly formed foam on the forward face of the wave covers much less area than the decaying foam in the wave's trough. Though perhaps not as dominant, some contribution to the azimuthal asymmetry of foam emissivity may also come from the different thickness of new and old foam. We continue to investigate these effects. Characterizing the azimuthal dependence of the microwave foam emissivity has the potential to improve the accuracy of wind vector retrievals from physically-based algorithms.

The change in ocean surface brightness temperature due to the presence of foam is an important parameter to be considered when modeling expected changes in brightness temperature that would be seen by down-looking radiometers on satellite or aircraft platforms. Figures 6 and 7 show predicted increases in ocean surface brightness temperature (at both 6.8 and 10.8 GHz and for H and V polarizations) using two different empirical parameterizations of foam fraction as a function of wind speed [2,7]. The increase in brightness temperature is calculated as

$$\Delta Tb = (f)(e_f - e_r)(T_w)$$

where f is foam fraction, T_w is the sea surface physical temperature, and e_f and e_r are the emissivities of foam and foam-free ocean surface rough water, respectively. Values of rough water emissivity were computed using the expressions given in Pandey and Kakar [8]; values of e_f are azimuthally averaged results taken from Figures 3 and 4.

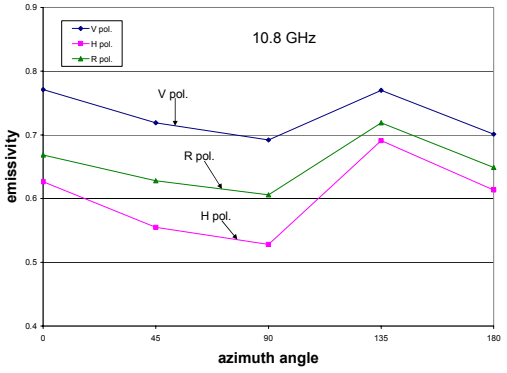

Figure 5. Foam emissivity at 10.8 GHz versus azimuth angle, for vertical, right circular, and horizontal polarizations.

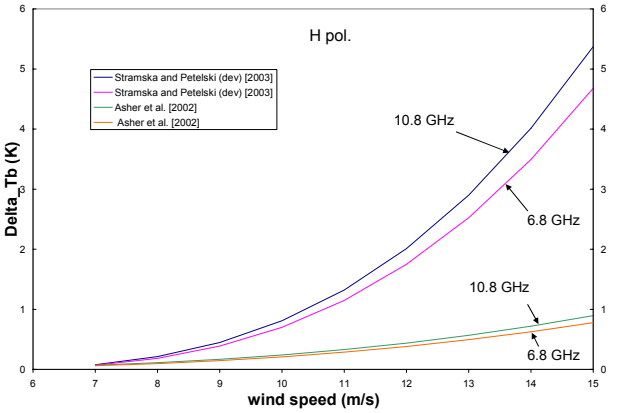

Figure 6. Predicted increase in ocean surface brightness temperature due to foam, using two different models of foam fraction as a function of wind speed [2,7], for horizontal polarization.

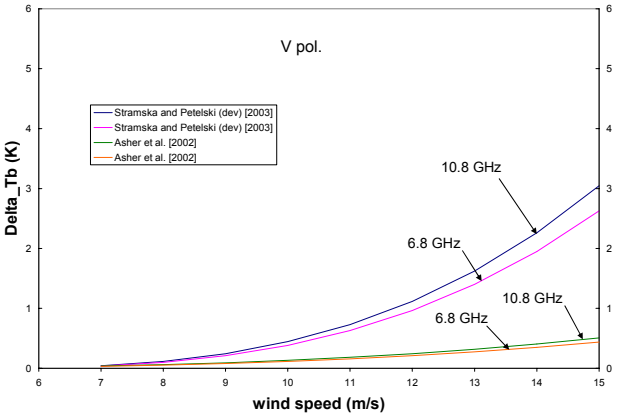

Figure 7. Same as Fig. 6 but for vertical polarization.

REFERENCES

[1] P.W. Gaiser, et al., "The WindSat spaceborne polarimetric microwave radiometer: Sensor description and early orbit performance," *IEEE Trans. Geosci. Rem. Sens*., vol. 42, no. 11, pp. 2347–2361, November 2004.

[2] W.E. Asher, J.B. Edson, W.R. McGillis, R. Wanninkhof, D.T. Ho, and T. Litchendorf, "Fractional area whitecap coverage and air-sea gas transfer during GasEx-98," in *Gas Transfer at Water Surfaces*, M.A. Donelan, W.M. Drennan, E.S. Saltzman, and R. Wanninkhof, eds., American Geophysical Union, Washington, DC, 199 - 204, 2002.

[3] L.A. Rose, W.E. Asher, S.C. Reising, P.W. Gaiser, K.M. St. Germain, D.J. Dowgiallo, K.A. Horgan, G. Farquharson, and E. J. Knapp, "Radiometric measurements of the microwave emissivity of foam," *IEEE Trans. Geosci. Remote Sens.* 40(12), 2619-2625, (2002).

[4] M.A. Aziz, S.C. Reising, W.E. Asher, L.A. Rose, P.W. Gaiser, and K.A. Horgan, "Effects of air-sea interaction parameters on ocean surface microwave emission at 10 and 37 GHz," *IEEE Trans. Geosci. Remote Sensing*, vol. 43, pp. 1763-1774, August 2005.

[5] S. Padmanabhan, S.C. Reising, W.E. Asher, L.A. Rose, and P.W. Gaiser, "Effects of foam on ocean surface microwave emission inferred from radiometric observations of reproducible breaking waves," *IEEE Trans. Geosci. Remote Sensing*, in press, October 2005.

[6] W.E. Asher and R. Wanninkhof, "The effect of bubble mediated gas transfer on purposeful dual gaseous experiments," *J. Geosphys. Res*., vol. 103, no. 10 pp. 555-560, May 1998.

[7] M. Stramska and T. Petelski, "Observations of oceanic whitecaps in the north polar waters of the Atlantic," *J. Geophys. Res*. vol 108, no. C3, 31-1 – 31-10, 2003.

[8] P. C. Pandey and R. K. Kakar, "An empirical emissivity model for a foam-covered sea," *J. of Oceanic Engineering*, vol. OE-7, No. 3, pp. 135-140, July 1982.